Comparative histomorphometric study of intraepithelial papillary capillaries on lichen planus, leukoplakia and squamous cell carcinoma of the oral mucosa

（口腔における扁平苔癬、白板症および扁平上皮癌の上皮乳頭内ループ状毛細血管の組織形態計測学的比較研究）

日本大学大学院松戸歯学研究科歯学専攻

長谷川　一弘

（指導　：　久山　佳代　教授）

This paper is a summary thesis of

Kazuhiro Hasegawa, Hiroyuki Sakamaki, Masahiro Higuchi et al., Histomorphometric Evaluation of Intraepithelial Papillary Capillaries in Oral Lichen Planus: A Histopathological Study, J Dermatol Res,2018, 4, 058. DOI: 10.23937/2469-5750/1510058

and

Kazuhiro Hasegawa, Hiroyuki Sakamaki, Masahiro Higuchi et al., Comparative histomorphometric study of intraepithelial papillary capillaries on leukoplakia with/without different dysplastic grading and squamous cell carcinoma of the oral mucosa, Oral Cancer, 2：37-44, 2018 https://doi.org/10.1007/s41548-018-0007-y

Abstract

Purpose: Oral lichen planus (OLP) and leukoplakia were included as an oral potentially malignant disorders (OPMDs), defined as clinical presentation carrying a risk of cancer development in the oral cavity in the new World Health Organization Classification of head and neck tumors. Diagnosis based on histopathological features is important for planning treatment. However, microvascular appearance was not regarding highly to pathological diagnosis. To analyze changes of intraepithelial papillary capillary loop (IPCL) patterns as the utility for pathological diagnosis, IPCLs of OLP, leukoplakias (histologically squamous cell hyperplasia, with low-or high-grade dysplasia, and oral squamous cell carcinoma (OSCC)) had performed.

Methods: Subjects for study 1 were selected from 42 cases (9 males, 33 females, 64.6 ± 9.1 years) clinico-histopathologically diagnosed as OLPs. Subjects for study 2, 40 cases (21 males, 19 females, average age 58.6 ± 3.8 years) clinically diagnosed as leukoplakias, histologically consisted 5 groups; each 10 of squamous cell hyperplasia, low- or high-grade dysplasia, OSCC (study 2) were selected. And normal mucosae were used as control in both studies. The IPCLs morphological measurements were performed in sites adjacent to the lesion, prominent areas and erosive areas of OLP (study 1) and the most prominent part of the lesion (study 2). The indexes of microvascular morphology were average areas and capillary loop angles (study 1), the area, shortest diameter, proximity to the basement membrane and circularity (study 2) were measured using Win Roof version 3.4 and ImageJ (Mitani Corporation, NIH) under microscopic observation. Statistical analyses were done by Kruskal–Wallis and Steel–Dwass tests. Values of $p < 0.05$ were considered significant.

Results: In study 1, area of IPCLs was larger than those in prominent areas of OLP ($p<0.001$). Capillary loop angles were 26.6 ± 19.3°, 84.5 ± 17.8°, 30.2 ± 22.4°, and 34.4 ±

19.3° for normal mucosa, sites adjacent to the lesion, prominent areas of OLP and erosive areas, respectively. Significant differences were observed between normal mucosa/prominent areas of OLP and site adjacent to the lesion ($p<0.001$). IPCL angle tended to be larger at sites adjacent to the lesion than at the erosive areas. Characteristic IPCL patterns were identified in the present study despite reticular/erosive type. In study 2, larger vessel diameter/areas, more extension and smaller circularity with dysplastic grading were observed, and OSCC showed the most prominent of them. In short, the changes in vessels of IPCLs in high-grade dysplasia and OSCC involve two factors: increased vessel diameter and prolongation of IPCLs toward the surface.

Conclusions: Characteristic and change of IPCL patterns in this research thus suggested the utility of pathological diagnostic criteria of OLP, leukoplakia and OSCC.

Key words: Oral lichen planus, leukoplakia, Oral squamous cell carcinoma, Oral potentially malignant disorders, intraepithelial papillary capillary loop

Introduction

Oral potentially malignant disorders (OPMDs) are defined as clinical presentation carrying a risk of development to OSCC, according to the new WHO classification of head and neck tumors [1]. Since many conditions that exhibit clinically hyperkeratosis on the oral mucosae, the clinical oral examination of oral mucosal lesions including oral lichen planus (OLP), leukoplakia with/without different dysplastic grading, and oral squamous cell carcinoma (OSCC) has limitation to predictive of pathological diagnosis [2].

OLP is a chronic inflammatory disease without a clear pathogenesis [3], and the diagnosis of OLP is based on both clinical and histopathological features. OLP clinically shows six classical clinical presentations, as described in the literature [4]: reticular, erosive, atrophic, plaque-like, papular and bullous. In contrast, results of biopsy should be described, particularly when white striae are ill defined, plaques are present, or regions appear in any other way unusual [5]. Even though clinical and histopathological standardized criteria for OLP have been unified [6], the potential for disagreement between clinical and histopathological diagnosis has been discussed for various other disorders clinically resemble OLP [3].

Oral leukoplakia is a clinical term used to describe white plaques is the most common potential malignant disorder of the oral mucosa [7]. This is the manifestation of hyperkeratotic white plaques with or without histologically changes of the squamous epithelium, including dysplasia and invasive carcinoma. Presence of oral epithelial dysplasia is the most important prognostic factor for malignant transformation of leukoplakia, but a specific clinical appearance is not usually apparent [8]. The degree of dysplasia or carcinoma in every case of leukoplakia can be hard to determine before biopsy [2].

Whereas, they were included in OPMDs in WHO 2017 [9], and the clinical significance of these early detection is very valuable. One approach to overcoming this problem is endoscopic narrow-band imaging (NBI), an optical image enhancement technology that enhances the contours and patterns of vessels in the mucosa surface by employing the characteristics of the light spectrum. Superficial blood vessels in the lamina propria mucosae are branching vessels that immediately extend horizontally; forming single loops referred to as intraepithelial papillary capillary loops (IPCLs) [10]. Lots of clinicals studies using NBI of dysplasia with oral leukoplakia and OSCC has been described [11-14]. Argument is also left in observation in NBI to oral lesion with keratinization, the study to histopathological microvascular architectures is necessary anyway. However, the microvascular appearance has not been regarded as highly relevant to the pathological diagnosis of OLP, oral leukoplakia and OSCC, and the histomorphological characteristics of IPCL have yet to be clarified.

The present study therefore undertook a comparative histomorphometric analysis of IPCLs in OLP, Leukoplakia and OSCC to investigate the potential for use as diagnostic criteria.

Material and Methods

1. Subjects

Subjects were selected from the pathology files of the Department of Oral Pathology at Nihon University School of Dentistry at Matsudo.

(1) Study 1 (OLP)

The characteristics of subjects in this study are summarized in Table 1. Forty-two patients with OLP (9 males, 33 females, 64.6 ± 9.1 years) were selected. The patients with clinical and histopathoalogically proven OLP cases according to diagnostic criteria [9,15], and the materials does not lack all macroscopic view record, digital pictures of oral cavity and biopsy specimen which comprised an area at the boundary part of the most prominent lesion and an adjacent area of normal mucosa, were included in the study. The normal oral mucosae were obtained through polypectomy from the perilesional areas of fibrous polyps without epithelial dysplasia to constitute the control group (5 males, 5 females; 7 buccal mucosae, 2 tongues, 1 gingiva).

Patients with history of exposure to dental materials, drugs etc. [16], any treatment for lichen planus or drugs associated with lichenoid reaction before biopsy, any malignant or viral involvement in mouth and pregnant women were excluded from the study sample.

(2) Study 2 (leukoplakia and OSCC)

The characteristics of subjects in this study are summarized in Table 2. Specifically, the 40 cases of clinically hyperkeratosis of gingivae (21 males, 19 females, 58.6 ± 3.8), which histologically constituted 10 cases of squamous cell hyperplasia (68.3 ± 9.5), 10 cases of low-grade dysplasia (66.3 ± 3.9), 10 cases of high-grade dysplasia (72.0 ± 7.3), and 10 cases of OSCC (74.6 ± 4.7). And mucous epithelium around fibro-epithelial polyps of gingivae after polypectomy was used for normal mucosa without inflammation (5 males, 5

females). Pre-operative examination identified no metastasis, including lymph node metastasis, and no patients had received prior anticancer treatment.

2. Gross findings

(1) Study 1 (OLP)

Oral examination was performed by the same oral surgeon for 42 patients, and a total of 96 sites were enrolled in the study, because patients with OLP at multiple sites were included. OLP was clinically diagnosed by the oral surgeon with well-defined looping and intersecting white lines/striae/patches with or without erosions and ulcerations [3,5,9,17].

1) Clinical examination

Classifications for the most prominent site were made by 2 oral surgeons and 3 oral pathologists based on Andreasen's 6 types and Brant's 2 types independently [18].

2) Biopsy specimens

Biopsy specimens were obtained for all 42 patients by the same oral surgeon, sampling an area at the boundary part of the most prominent lesion and an adjacent area of normal mucosa.

(2) Study 2 (leukoplakia and OSCC)

The 40 cases of clinically diagnosed as leukoplakia of gingivae by oral surgeons were clinically diagnosed.

1) Surgical specimens

Surgicopathologic specimens were obtained for all 40 patients at tumorectomy.

3. Histopathological and immunohistochemical specimens

Serial sections (each 4 μm thick) were prepared for hematoxylin and eosin (HE) and immunohistochemical staining. For immunohistochemical staining, the primary antibodies shown in Table 3 were used. For the detection of these proteins, the EnVision +Polymer

System (Dako, Glostrup, Denmark) was used following manufacture's protocol. Sections were developed in a solution of 3,3'-dianibobenzidine tetrahydrochloride. Finally, all sections were counterstained with Mayer's hematoxylin. Muscle tissue and granulation tissue were used as positive controls for CD34 and SMA, respectively. For evaluation of the immunohistochemical staining technique, mouse and rabbit universal g-negative controls (Dako) were used as negative controls during the staining procedure instead of primary antibodies.

4. Histopathologic criteria

(1) Study 1 (OLP)

Histologic specimens included in the study were selected according to definite histopathological criteria according to the American Academy of Oral and Maxillofacial pathology: ⅰ) presence of a well-defined band-like zone of cellular infiltration consisting mainly of lymphocytes in the superficial part of the connective tissue; and ⅱ) signs of "liquefaction degeneration" in the basal layer; and ⅲ) absence of epithelial dysplasia [15].

(2) Study 2 (leukoplakia and OSCC)

Degrees of epithelial dysplasia were determined according to WHO criteria [1]. In addition, cases accompanied by secondary inflammation with ulcer/erosion were excluded.

(3) Histopathologic and immunohistochemical diagnosis

Two or more oral pathologists blinded to the biopsy material made the histopathological diagnosis and the assessments of immunohistochemical staining. Histopathological and immunohistochemical evaluations were identical among 2 or more oral pathologists.

5. Evaluation of microvascular morphology

Sections with CD34 and SMA immunoreactivities (1 section each) were used to decide fields for microvascular morphological observation. After immunohistochemical observation, entire sections with CD34 and SMA reactivity were scanned microscopically at low power (×40) to identify hot spots, as the areas with the highest number of microvessels. Individual regional microvessels were then counted under high power (×200) and calculated as the average value ± standard deviation of 3 fields to evaluate microvascular morphology. The CD34/SMA positive vessel area was converted into a binary format image and changes in microvessel area and the morphology of microvascular in the submucosa were estimated. Morphological analyses were using Win Roof version 3.4 image analysis software (Mitani Corporation, Tokyo, Japan) and ImageJ (NIH).

(1) Morphological indexes

1) Study 1 (OLP)

ⅰ) Capillary loop angles: angle of the course of the capillaries to the virtual basal membrane (Fig. 1)

ⅱ) Average IPCL area: areas of IPCLS under the basement membrane

2) Study 2 (leukoplakia and OSCC)

ⅰ) Capillary shortest diameter: the smallest diameter between the medial surfaces of endothelial cell

ⅱ) Average IPCL area: areas of IPCLs under the basement membrane

ⅲ) The proximity to the basement membrane: the distance from the basilar membrane to the most epithelial side of the blood vessel, IPCL extend horizontally, and smaller proximity indicates extension of the loops.

ⅳ) Degree of circularity: irregularity of the vascular lumen, which is the relative ratio when making perfect circle 1.0 and a decline of the ratio means a rise of irregular degree

6. Statistical assessment

All statistical analyses were performed using SPSS for Windows version 14.OJ (IBM, Tokyo, Japan). Statistical analyses were performed using the Kruskal-Wallis test and Steel-Dwass test. Values of $P<0.05$ were considered significant.

Results

1. Study 1 (OLP)

(1) Clinico-pathological findings

The distribution of clinico-pathological findings is shown in Table 1. Details of the most prominent areas at 73 sites were the buccal mucosa in 70 (95.9%), lip in 2 (2.7%) and tongue in 1 (1.4%). Brant's classification was white in 43 (58.9%) and red in 30 (41.1%). Andreasen's classification was reticular in 60 (82.2%), erosive in 6 (8.2%), erosive +reticular in 5 (6.8%), atrophic in 1 (1.4%) and reticular and white patch in 1 (1.4%).

(2) Histopathological and immunohistochemical finding

Histopathological findings are provided in Table 4. Representative images of OLP and characteristic findings focused on IPCLs are shown in Figures 2 (a-f) and 3 (a1-d1, a2-d2), respectively. Appearance rates of histopathological characteristics were keratinization, 100.0%; frequent saw-toothed rete ridges, 69.0%; and Max Joseph spaces, 16.7%.

Figure 3 shows Microscopic images focused on IPCLs (HE; a1-d1, a2-d2) and immunohistochemical staining using SMA antibody (a3-d3). Regardless of the classification from clinical inspection, IPCLs ran obliquely to the basal membrane at the sites adjacent to the lesion (Fig. 3b1, 3b2).

(3) Evaluation of microvascular morphology

capillary loop angles (Fig. 4a) and Average areas (Fig. 4b) of normal mucosa, sites adjacent to the lesion, the most prominent areas of OLP, and erosive areas are shown in Figure 4. Mean Capillary loop angles were 26.6 ± 19.3°, 84.5 ± 1 7.8°, 30.2 ± 22.4°, and 34.4 ± 19.3° for normal mucosa, sites adjacent to the lesion, prominent areas of OLP and erosive areas, respectively. Significant differences were observed between normal

mucosa/prominent areas of OLP and site adjacent to the lesion ($p<0.001$). IPCL angle tended to be larger at sites adjacent to the lesion than at the erosive areas.

IPCL areas were 978.0 ± 523.7 μm^2, 1537.1 ± 1061.4 μm^2, 689.0 ± 351.9 μm^2 and 1092.1 ± 153.3 μm^2 for normal mucosa, sites adjacent to the lesion, prominent areas of OLP and erosive areas, respectively. Significant differences were observed between prominent areas of OLP and sites adjacent to the lesion ($p<0.001$). Area of IPCLs tended to be larger in sites adjacent to the lesion than in normal mucosa.

2. Study 2 (leukoplakia and OSCC)

(1) Histopathological and immunohistochemical finding

Representative images of normal gingival and mucosal lesions are shown in Fig. 5a1-e1). Microscopic images with immunohistochemical staining using CD34 antibody are shown in Fig. 5a2-e2: 200X, a3-e3: 400X. More IPCL extension toward the basal membrane and IPCL dilation with dysplastic grading, and OSCC showed the most prominent of them.

(2) Evaluation of microvascular morphology

Average capillary shortest diameter in normal, hyperplasia, low-grade dysplasia, high-grade dysplasia and OSCC groups were 8.79 ± 0.84, 9.29 ± 1.06, 21.15 ± 1.31, 23.98 ± 2.11 and 25.97 ± 2.13μm, respectively (Fig. 6a). A significant difference was seen among the 5 groups ($p<0.01$). Larger diameters were seen with high-grade dysplasia and OSCC when compared with normal mucosa and hyperplasia ($p<0.01$). Average IPCL areas in the 5 groups were 41.19 ± 1.90, 52.75 ± 3.64, 540.93 ± 189.92, 639.37 ± 173.53 and 848.33 ± 135.71μm^2, respectively, again showing a significant difference between groups ($p<0.01$) (Fig. 6b). Larger areas were shown with high-grade dysplasia and OSCC when compared with normal mucosa, and with OSCC when compared with hyperplasia ($p<0.01$, each).

Capillary vessels in low-grade dysplasia showed a larger area than in normal mucosa ($p<0.05$). The proximity to the basement membrane in the 5 groups was 19.78 ± 1.53, 16.36 ± 1.22, 14.51 ± 1.08, 12.03 ± 2.01 and 8.65 ± 2.00 ㎛, respectively (Fig. 6C). A significant difference was seen among the 5 groups ($p<0.01$). A lower degree of proximity to the basal membrane, that is, more extension of IPCL was observed in OSCC compared with normal mucosa and hyperplasia, and in high-grade dysplasia compared with normal mucosa ($p<0.01$). As a measure of irregularity of the vascular lumen, the degree of circularity in the 5 groups was 0.82 ± 0.04, 0.79 ± 0.03, 0.62 ± 0,07, 0.54 ± 0.05 and 0.43 ± 0.07, respectively (Fig. 6d). A significant difference was seen among the 5 groups ($p<0.01$). Smaller circularity was shown in high-grade dysplasia and OSCC compared with normal mucosa and hyperplasia ($p<0.05$).

Discussion

The clinical condition of OLP changes according to disease progression and its site. Patients presenting with mucosal alterations and a region distribution fully consistent with OLP may thus only require a single tissue sample for histopathological evaluation. Conversely, the number of tissue samples to be obtained is guided by several considerations. Besides, histopathological cases of "suspected OLP" lack the characteristic features of "liquefaction degeneration in the basal cell layer" and "Civatte body formation". In addition, termed "interface mucositis," which is also encountered in oral regions of lupus erythematosus and in additional oral lichenoid conditions [19,20]. Namely pathological diagnosis of OLP is difficult, particularly clinically diagnosed erosive OLP [21].

The precision of diagnosis is therefore regarded for these reasons as a problem in OLP biopsy, and supplementary examination methods are needed. Concerning the histopathological evaluation of microvessels, some studies have evaluated microcirculation characteristics in the presence of OLP [22-27]. Microvessel density in OLP regions was observed to be significantly higher than in control specimens in previous studies [26,27]. However, López de Blanc et al reported the number of blood vessels was not increased, but the increased vessels area indicated that OLP is a more congestive region [25].

Regarding the relationship between IPCL and clinical condition of OLP, angiogenesis and expression of vascular endothelial growth factor correlated closely with the different clinical forms of OLP regions [28-30]. However, no histopathological studies appear to have examined the morphology and course of IPCLs in OLP. In the present study, average capillary angle and area is much higher between normal and sites adjacent to the lesion and not between normal and prominent/erosive areas. In prominent/erosive areas, epithelial regeneration starts from basal cells located near the erosion/ulcer caused

by chronic inflammation, and granulation tissue is formed in the mesenchymal tissue. Therefore, small new vessels and elongated IPCLs by congestion were intermingled for tissue repair. Meanwhile, IPCLs around those pathological changes were expanded and ran obliquely in both reticular and erosive types of prominent areas. IPCLs in neighboring normal areas might extend and supply the prominent areas with oxygen. In addition, thirteen cases in this study showed microhemorrhages on histological examination. Erythrocytes were conjectured to have leaked due to dilation and hyperpermeability of IPCLs.

OLP shows histopathologically non-specific inflammatory changes under clinical conditions, and the pathological diagnostic criteria need to be discussed. By contrast, IPCLs are expanded and run obliquely to the basal membrane at the sites adjacent to the lesion. Consequently, characteristic IPCL patterns were identified in the present study irrespective of the reticular/erosive type, indicating the utility of IPCL patterns as the pathological diagnostic criteria.

Generally, intraepithelial squamous dysplasia may progress to carcinoma in situ and eventually to invasive carcinoma, and the higher the grade of dysplasia, the greater the likelihood of progression to malignancy [31]. To judge the presence of dysplasia and/or OSCC before biopsy, changes in IPCL patterns as observed under NBI have started to be studied for oral leukoplakia [13,32,33]. Usefulness of NBI to detection of squamous precursor lesions and early-stage SCC in the oral cavity was described in the previous studies [11-13,32]. Studies of IPCL morphology by histopathological image analysis using resection materials are scarce for oral lesions, even though blood vessel numbers and densities with progress in the grade of dysplasia have been discussed [34,35]. Incidentally, oral mucosae have some particularities, such as, height subepithelial papilla, keratinization

degree different depending on parts and without muscularis. The study to histopathological microvascular architectures isn't enough, though arguments are also left in observation by NBI to oral lesion with keratinization. However, keratotic whitish lesion frequently concealed macroscopic diagnosis. [12,32,36]. Clinical hyperkeratosis was selected in this study to analyze IPCL morphological change under the keratotic oral mucosae. In short, changes in vessels of IPCLs in high-grade dysplasia and OSCC involved two main factors: increased vessel caliber and prolongation of IPCLs toward the surface. Histomorphological results of the present study could not admit contradiction with NBI's findings of oral leukoplakia and OSCC in the previous studies [13,32,33]. These vascular changes were assumed to be associated with increased atypia of blood vessels [10]. Alterations in microvascular structures represented by IPCL irregularities occurred with architectural or cytological abnormalities in squamous epithelial lesions. An increase in blood supply is necessary for any type of epithelial proliferation [37,38]. Since IPCLs are located near the epithelial basement membrane, changes in IPCL patterns are thought to reflect alterations in the structures of the epithelial basal layer.

Regarding IPCL, in the first step, IPCLs with dilation arise during basal cell hyperplasia, then expand and elongate in low-grade dysplasia. Next, microvascular irregularities with branching of IPCLs are observed in high-grade dysplasia and OSCC in this study. In this study, 2 kinds of blood vessels should be intermingled in the surface observed; normal IPCL with expanded and extended change which exists in the lamina propria mucosa and juvenile IPCL like blood vessels led by neovascularization in high-grade dysplasia and early invasive squamous cell carcinoma. The change of IPCL patterns can be of help in detecting oral leukoplakia with higher grade dysplasia or invasive carcinoma.

In conclusion, IPCLs are extended and run obliquely to the basal membrane at the sites adjacent to the lesion of OLP in study 1. Besides, characteristic IPCL patterns were identified despite reticular/erosive. In study 2 of leukoplakia and OSCC, the microvascular irregularity and proliferation composed by IPCLs and IPCL like abnormal capillaries were observed pathologically in squamous epithelial lesions of the oral cavity. The changes in vessels of IPCLs in high-grade dysplasia and OSCC involve two factors: increased vessel diameter and prolongation of IPCLs toward the surface.

This research thus suggested the utility of these patterns in pathological diagnostic criteria.

Reference

1. Pieter JS (2017) International agency for research on cancer (IARC), WHO classification of head and neck tumours, Lyon

2. Epstein JB, Güneri P, Boyacioglu H, Abt E (2012) The limitations of the clinical oral examination in detecting dysplastic oral lesions and oral squamous cell carcinoma. J Am Dent Assoc 143:1332-1342.

3, Van der Meij EH, Schepman KP, Van der Waal I (2003) The possible premalignant character of oral lichen planus and oral lichenoid lesions: A prospective study. Oral Surg Oral Med Oral Pathol Oral Radiol Endod 96: 164-171.

4. Andreasen JO (1968) Oral lichen planus: a clinical evaluation of 115 cases. Oral Surg Oral Med Oral Pathol 25: 31-41.

5. Cawson RA, Odell EW (1998) Disease of the oral mucosa: Non-infective stomatitis. In: Cawson RA, Odell EW (eds) Essentials of oral pathology and oral medicine. 6th ed. London: 187-191.

6. Van Der Meij EH, Van Der Waal I (2003) Lack of clinicopathologic correlation in the diagnosis of oral lichen planus based on the presently available diagnostic criteria and suggestions for modifications. J Oral Pathol Med 32: 507-512.

7. Lodi G, Porter S (2008) Management of potentially malignant disorders: Evidence and critique. J Oral Pathol Med 37:63-69.

8. Lee JJ, Hung HC, Cheng SJ, Chen YJ, Chiang CP, et al. (2006) Carcinoma and dysplasia in oral leukoplakias in Taiwan: Prevalence and risk factors. Oral Surg Oral Med Oral Pathol Oral Radiol Endod 101:472-480.

9. Reibel J, Tilakaratne WM, Gale N, Westra WH, Hille J, et al. (2017) Oral potentially malignant disorders and oral epithelial dysplasia. In: El-Naggar AK, Chan JKC, Grandis JR, et al. (eds) *WHO classification of head and neck tumours*.

10. Kaga M, Inoue H, Kudo SE, Hamatani S (2011) Microvascular architecture of early esophageal neoplasia. Oncol Rep 26:1063-1067.

11. Takano JH, Yakushiji T, Kamiyama I, Nomura T, Katakura A, et al. (2010) Detecting early oral cancer: Narrowband imaging system observation of the oral mucosa microvasculature. Int J Oral Maxillofac Surg 39: 208-213.

12. Yang SW, Lee YS, Chang LC, Hwang CC, Chen TA (2012) Diagnostic significance of narrow-band imaging for detecting high-grade dysplasia, carcinoma in situ, and carcinoma in oral leukoplakia. Laryngoscope 122:2754-2761.

13. Yang SW, Lee YS, Chang LC, Chien HP, Chen TA (2012) Clinical appraisal of endoscopy with narrow-band imaging system in the evaluation and management of homogeneous oral leukoplakia. ORL 74:102-109.

14. Vu AN, Farah CS (2014) Efficacy of narrow band imaging for detection and surveillance of potentially malignant and malignant lesions in the oral cavity and oropharynx: A systematic review. Oral Oncol 50:413-420.

15. Van der Meij EH, Mast H, Van der Waal I (2007) The possible premalignant character of oral lichen planus and oral lichenoid lesions: a prospective five-year follow-up study of 192 patients. Oral Oncol 43: 742-748.

16. Thornhill MH, Sankar V, Xu XJ, Barrett AW, High AS, et al. (2006) The role of histopathological characteristics in distinguishing amalgamassociated oral lichenoid reactions and oral lichen planus. J Oral Pathol Med 35: 233-240.

17. Al-Hashimi I, Schifter M, Lockhart PB, Wray D, Brennan M, et al. (2007) Oral lichen planus and oral lichenoid lesions: Diagnostic and therapeutic considerations. Oral Surg Oral Med Oral Pathol Oral Radiol Endod 103 (suppl S25): e1-e12.

18. Brant JM, Vasconcelos AC, Rodrigues LV (2008) Role of apoptosis in erosive and reticular oral lichen planus exhibiting variable epithelial thickness. Braz Dent J 19: 179-185.

19. Patterson JW (2016) The lichenoid reaction pattern ("interface dermatitis"). In: Patterson JW (ed) Weedon's Skin Pathology. 4th ed. London: Churchill Livingston Elsevier; 39.

20. Khudhur AS, Di Zenzo G, Carrozzo M (2014) Oral lichenoid tissue reactions: Diagnosis and classification. Expert Rev Mol Diagn 14: 169-184.

21. Sakurai J, Okada N, Omura K (2011) The correlation between clinical and histopathological diagnosis of oral lichen planus. JJOMM 17: 39-43.

22. Bamberger ES, Perrett CW (2002) Angiogenesis in benign, pre-malignant and malignant vulvar lesions. Anticancer Res 22: 3853-3865.

23. Ben-Av P, Crofford LJ, Wilder RL, Hla T (1995) Induction of vascular endothelial growth factor expression in synovial fibroblast by prostaglandin E and interleukin-1: A potential mechanism for inflammatory angiogenesis. FEBS Lett 372: 83-87.

24. Forsythe JA, Jiang BH, Iyer NV, Agani F, Leung SW, et al. (1996) Activation of vascular growth factor gene transcription by hypoxia-inducible factor 1. Mol Cell Biol 16: 4604-4613.

25. López de Blanc S, Gendelman H, Itoiz ME, Lanfranchi H (1996) Study of vascular pattern in oral lichen planus. Acta Odontol Latinoam 9: 27-36.

26. Jin Y, Tipoe GL, White FH, Yang L. (1995) A quantitative investigation of immunocytochemically stained blood vessels in normal, benign, premalignant and malignant human oral cheek epithelium. Virchows Arch 427: 145-151.

27. Tipoe GL, Jin Y, White FH (1996) The relationship between vascularity and cell proliferation in human normal and pathological lesions of the oral cheek epithelium. Eur J Cancer B Oral Oncol 32B: 24-31.

28. Mittal N, Shankari GM, Palaskar S (2012) Role of angiogenesis in the pathogenesis of oral lichen planus. J Oral Maxillofac Pathol 16: 45-48.

29. Tao X, Huang Y, Li R, Qing R, Ma L, et al. (2007) Assessment of local angiogenesis and vascular endothelial growth factor in the patients with atrophic-erosive and reticular oral lichen planus. Oral Surg Oral Med Oral Pathol Oral Radiol Endod 103: 661-669.

30. Hazzaa HH, El-Wakeel NM, Attia EA, Abo Hager EA (2016) ALK1 expression in oral lichen planus: A possible relation to microvessel density. Oral Pathol Med 45: 373-380.

31. Wamakulasuriya S, Reibel J, Bouquot J, Dabelsteen E (2008) Oral epithelial dysplasia classification systems: Predictive value, utility, weakness and scope for improvement. J Oral pathol Med 37:127-133.

32. Yang SW, Lee YS, Chang LC, Hwang CC, Luo CM, Chen TA (2012) Use of endoscopy with narrow band imaging system in evaluating oral leukoplakia. Head Neck 34:1015-1022.

33. Yang SW, Lee YS, Chang LC, Hsieh TY, Chen TA (2013) Implications of morphologic patterns of intraepithelial microvasculature observed by narrow-band imaging system in cases of oral squamous cell carcinoma. Oral Oncol 49: 86-92.

34. Yokoyama M (2011) Alterations in stromal reaction during tumor progression in oral mucosa. J Hard Tissue Biol 20: 23-30.

35. Jyothsna M, Rammanohar M, Kumar K (2017) Histomorphometric analysis of angiogenesis using CD31 immunomarker and mast cell density in oral premalignant and malignant lesions: A pilot study. J Clin Diagn Res 11: ZC37-ZC40.

36. Vu AN, Matias M, Farah CS (2015) Diagnostic accuracy of narrow band imaging for detection of oral potentially malignant disorders. Oral Dis 21:519-529.

37. Viacava P, Naccarato AG, Bocci G, Fanelli G, Aretini P, Lonobile A, Evangelista G, Montruccoli G, Bevilacqua G (2004) Angiogenesis and VEGF expression in pre-invasive lesions of the human breast. J Pathol 204:140-146.

38. Fujii S, Yamazaki M, Muto M, Ochiai (2010) A microvascular irregularities are associated with composition of squamous epithelial lesions and correlate with subepithelial invasion of superficial-type pharyngeal squamous cell carcinoma. Histopathology 56: 510-522.

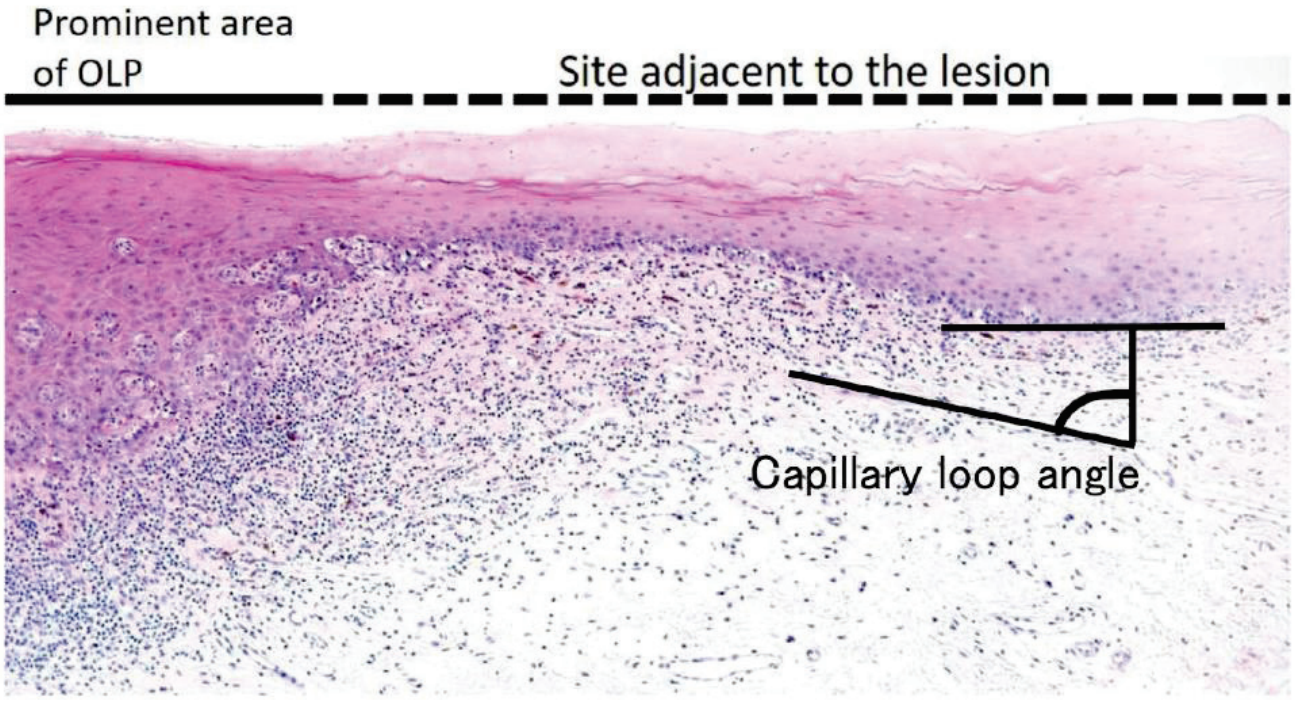
Prominent area
of OLP
Site adjacent to the lesion
Capillary loop angle

Fig.1

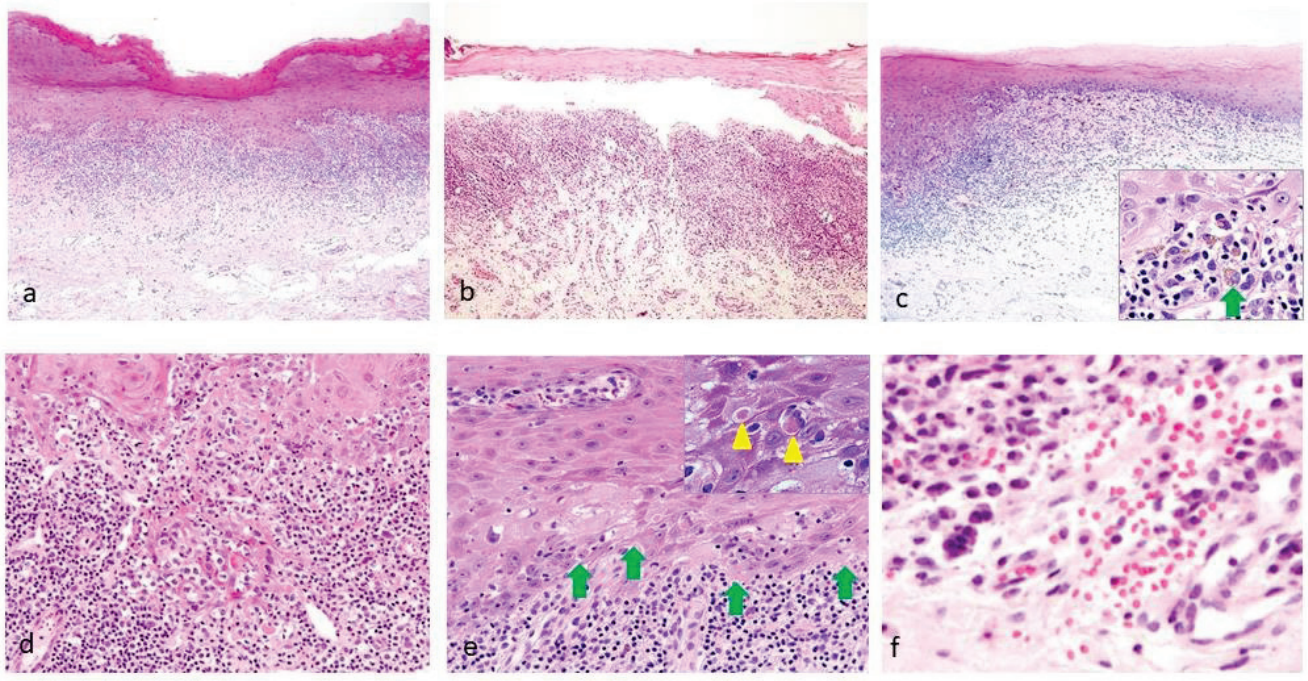
a
b
c
d
e
f

Fig.2

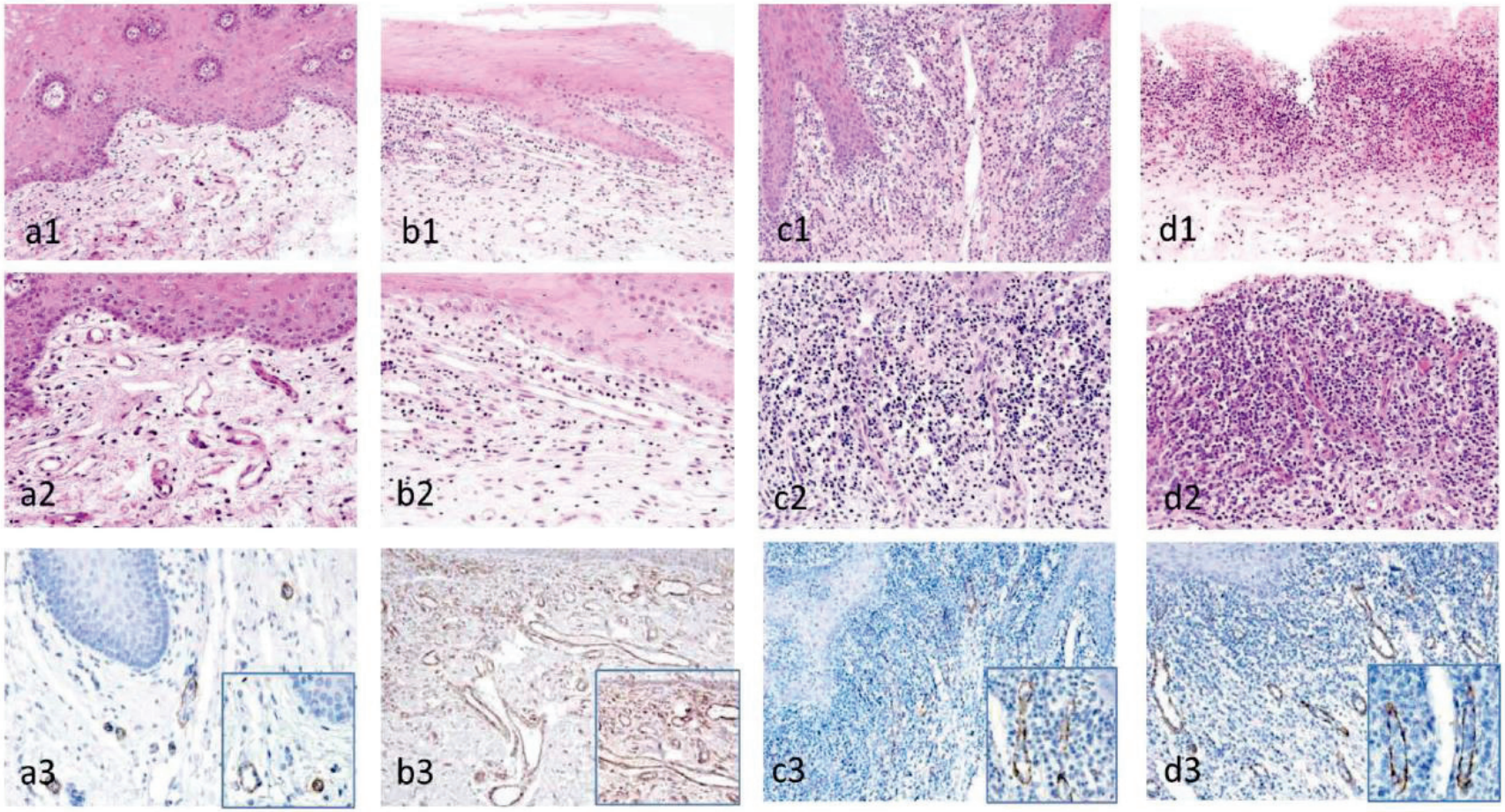

Fig.3

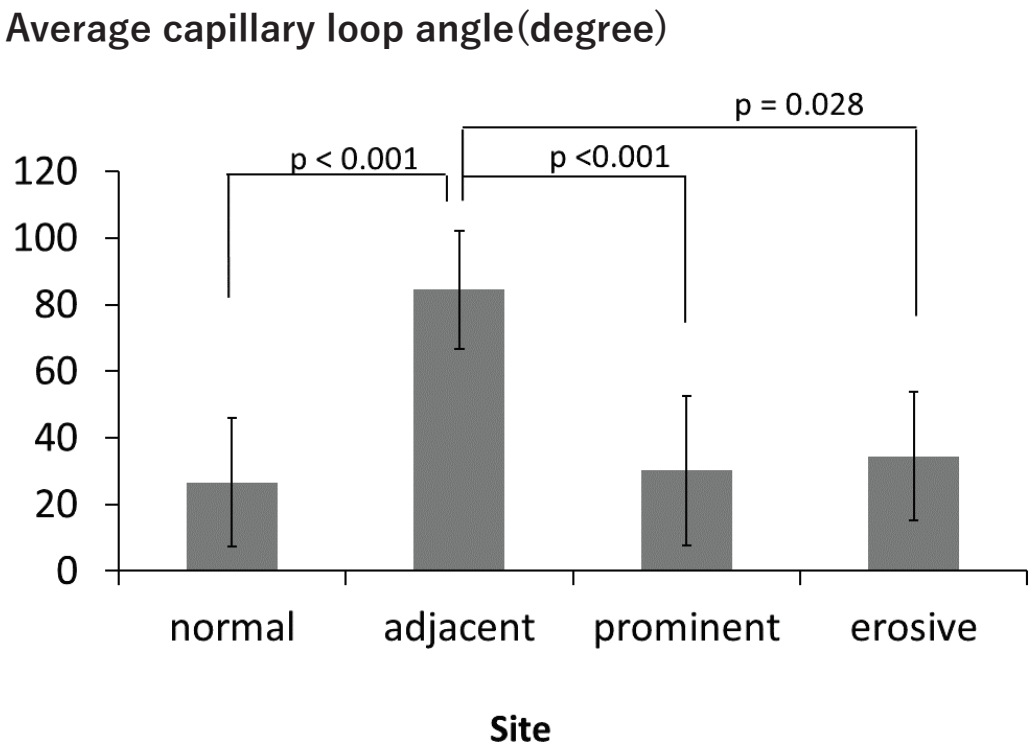
Average capillary loop angle(degree)
p = 0.028
p < 0.001
p <0.001
120
100
80
60
40
20
0
normal
adjacent
prominent
erosive
Site

Fig.4-a

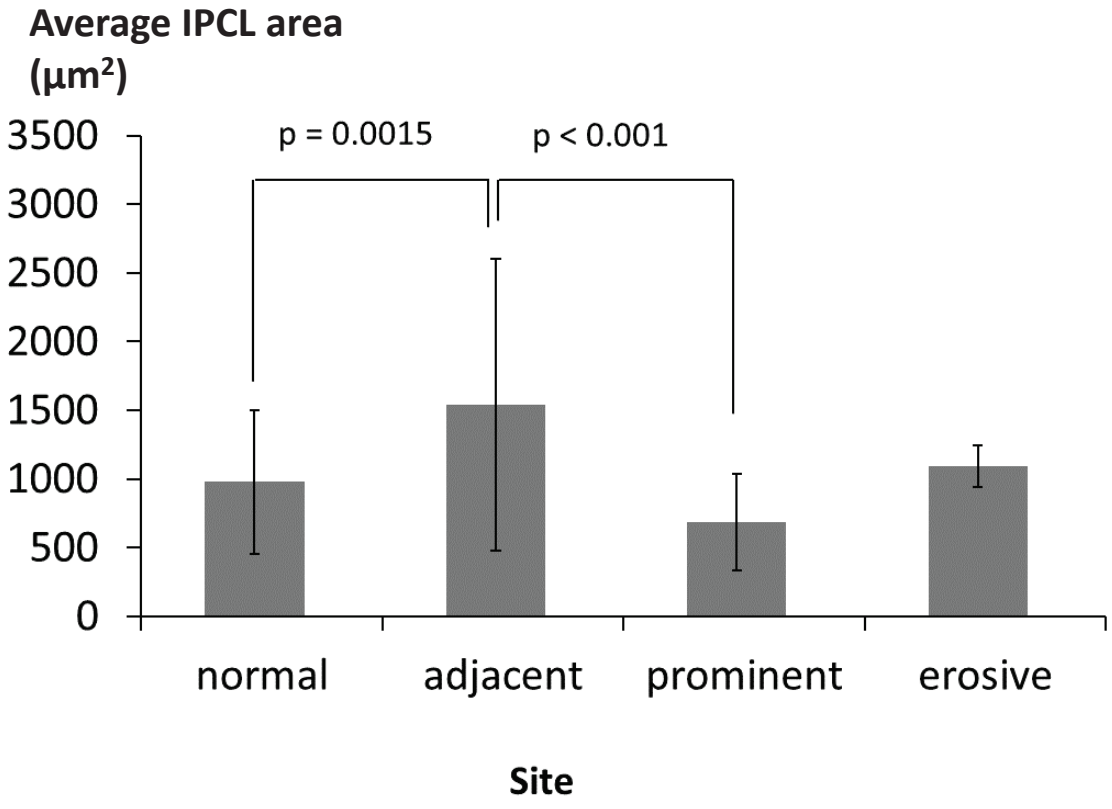
Average IPCL area
(μm²)
p = 0.0015
p < 0.001
3500
3000
2500
2000
1500
1000
500
0
normal
adjacent
prominent
erosive
Site

Fig.4-b

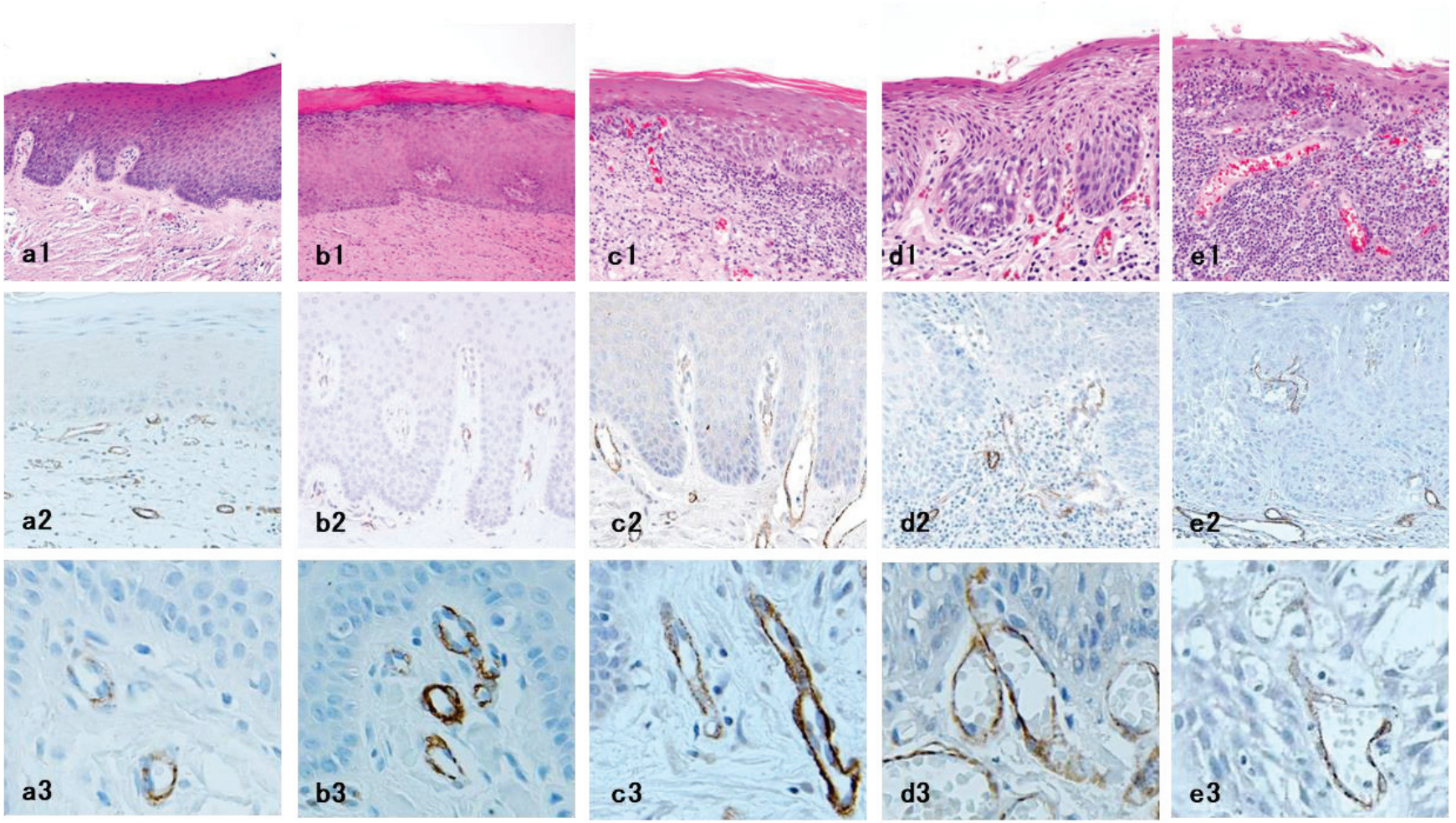

Fig.5

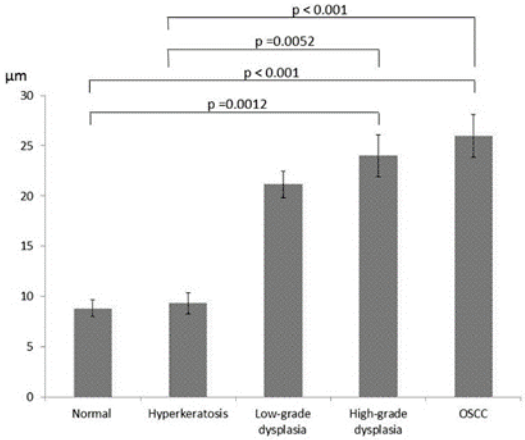

a capillary shortest diameter

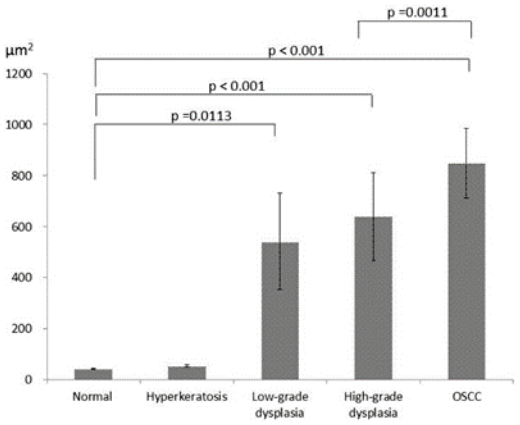

b areas of capillary vessels

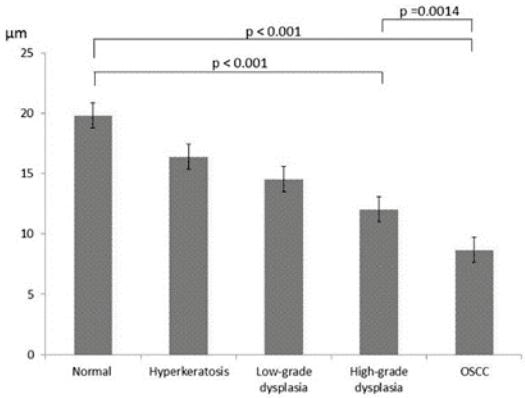

c the proximity to the basement membrane

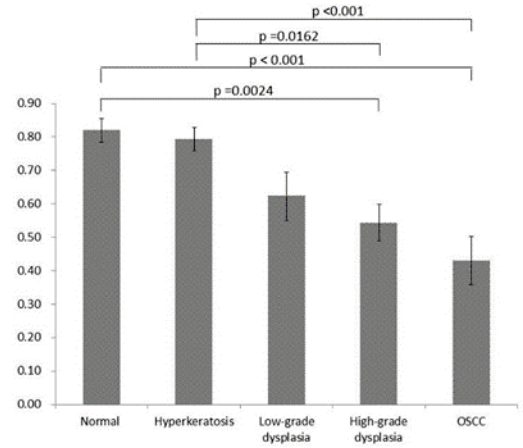

d degree of circularity

Fig.6

Figure Legends

Figure 1: Represented capillary loop angle in the site adjacent to the prominent are of OLP (HE, ×4).

Figure 2: Characteristic histopathological findings of oral lichen planus (HE). a) Surface is covered by hyperkeratotic stratified squamous cells with saw-toothed rete ridges, and band-like lymphoplasmacytic cells are seen infiltrating at the epithelia-mesenchymal junction (×10); b) Max Joseph spaces are observed (×10); c) Surface is covered by thinning and flattening of the epithelium with band-like lymphocytic infiltration (×10). Arrow, melanophores (×60, in the square); d) Fibrin and granulating connective tissue exist in the floor of the erosive lesion (×60); e) Liquefaction degeneration in basal cells at the epithelio-mesenchymal junction is evident (arrows), and Civatte bodies exist at the bottom of the epithelial layer (arrowhead) (×60); f) Micro-hemorrhages around IPCLs (×100).

Figure 3: Images focused on IPCLs. a) Normal mucosa: 1) Small IPCLs in the submucosa (HE, ×20); 2) Slight infiltration of lymphocytes and round IPCL (HE, ×40); 3) Small IPCLs with positive staining for SMA (SMA, ×40), and high-power magnification in the square (SMA, ×60). b) Sites adjacent to the lesion: 1) Elongated/slightly expanded IPCLs run at an angle to the basal membrane in the sites adjacent to the lesion (HE, ×20); 2) IPCL area is bigger than normal and prominent areas (HE, ×40); 3) Elongated/slightly expanded IPCLs staining positive for SMA (SMA, ×40), with high-power field shown in the square (SMA, ×60). c) Main lesion with keratotic epithelium: 1) Elongated IPCLs are prominent, and run vertically to the basal membrane (HE, ×20); 2) Strong infiltration of lymphocytes and swelling of endothelial cells of IPCLs (HE, ×40); 3) Elongated IPCLs run vertically with positive for SMA (SMA, ×40), and high-power field in the square (SMA, ×60). d) Erosive main lesion: 1) Elongated IPCLs are prominent, and run vertical to the basal membrane (HE, ×20); 2) Strong infiltration of lymphocytes and swelling of endothelial cells of IPCLs (HE, ×40); 3) Expanded IPCLs are prominent, and run vertical to the basal membrane (SMA, ×40), with high-power field shown in the square (SMA, ×60).

Figure 4: Results of IPCL histomorphometrical evaluation of oral lichen planus (normal: Normal mucosa, adjacent: Sites adjacent to the lesion, prominent: The most prominent areas, erosive: Erosive areas). a) Average capillary loop angles of IPCLs in normal mucosa and lichen planus. b) Average IPCL area of normal mucosa and lichen planus.

Figure 5: Representative HE images of gingival mucosa and oral mucosal lesions are shown in a1–e1 (×20). Microscopic images with immunohistochemical staining using CD34 antibody are shown in a2–e3 (a2–e2;×20, a3–e3;×40). a1 Normal stratified squamous epithelium with keratinization in normal gingival mucosa. b1 A thickened keratinized layer with acanthosis and without cellular atypia in hyperplasia. c1 Architectural disturbance accompanied by minimal to moderate cellular atypia limited to the lower third to middle of the epithelium in low-grade dysplasia. d1 Greater than two-thirds of the epithelium showed architectural disturbance associated with moderate to severe cellular atypia in high-grade dysplasia. e1 Cancer cells with squamous cell characteristics had proliferated and invaded into the superficial submucosal zone in oral squamous cell carcinoma (OSCC). a2, 3 small rounded capillaries were observed under the epithelium in gingival mucosa. b2, 3 Circularity with slightly expanded capillaries were observed in hyperplasia. c2, 3 Intraepithelial papillary capillary loop (IPCL) extension toward the basal membrane and IPCL dilation were seen in low-grade dysplasia. d2, 3 IPCLs with dilation and irregular form had shown just below the epithelium in high-grade dysplasia. e2, 3 IPCL abnormalities were clearly recognizable, and moreover, marked IPCL proliferation with irregular branching was observed in the tumor stroma of OSCC.

Figure 6: Evaluation of IPCL irregularity among five groups. (Normal, squamous cell hyperplasia, low-grade dysplasia, high-grade dysplasia, OSCC)

Table 1 Clinico-pathological characteristics of all cases (Study 1: Oral lichen planus)

Case	Age	Sex	Clinicopathological findings												
			Affected lesion			Macroscopic findings									
			Main lesion site		Anoter lesion site	No.Sites*	Brant JM's classification				Andreasen's classification				Biopsy site
1	49	M	left sides	buccal mucosa		1			left	red			left	erosive	left buccal mucosa
2	61	M	both sides	buccal mucosa		2	right	red	left	red	right	erosive	left	reticular	right buccal mucosa
3	60	M	both sides	buccal mucosa		2	right	white	left	white	right	reticular	left	reticular	left buccal mucosa
4	36	M	both sides	buccal mucosa		2	right	white	left	white	right	reticular	left	reticular	right buccal mucosa
5	68	M	both sides	buccal mucosa		2	right	red	left	white	right	reticular and erosive	left	reticular	left buccal mucosa
6	62	M	left side	buccal mucosa		1			left	white			left	reticular	left buccal mucosa
7	59	M	both sides	buccal mucosa	left lateral border of tongue	3	right	white	left	red	right	reticular	left	reticular	left buccal mucosa
8	76	M	right side	buccal mucosa		1	right	red			right	reticular			right buccal mucosa
9	71	M	both sides	buccal mucosa		2	right	white	left	white	right	reticular	left	reticular	left buccal mucosa
10	58	F	both sides	buccal mucosa		2	right	white	left	red	right	reticular and white patch	left	reticular and erosive	right buccal mucosa
11	64	F	right side	lateral border of tongue		1	right	white			right	reticular			lateral border of tongue
12	69	F		lower lip		1		red				reticular			lower lip
13	69	F	both sides	buccal mucosa	both lateral border of tongue	4	right	white	left	white	right	reticular	left	reticular	lateral border of tongue
14	71	F	left side	buccal mucosa		1			left	white			left	reticular	left buccal mucosa
15	67	F	both sides	buccal mucosa	upper both sides of gingiva	4	right	white	left	white	right	reticular	left	reticular	left buccal mucosa
16	64	F	both sides	buccal mucosa		2	right	red	left	white	right	erosive	left	reticular	right buccal mucosa
17	70	F	both sides	buccal mucosa	lower both sides of gingiva	4	right	white	left	white	right	reticular	left	reticular	gingiva
18	70	F	both sides	buccal mucosa		2	right	white	left	white	right	reticular	left	reticular	left buccal mucosa
19	70	F	both sides	buccal mucosa		2	right	white	left	white	right	reticular	left	reticular	right buccal mucosa
20	63	F	both sides	buccal mucosa		2	right	white	left	white	right	reticular	left	reticular	left buccal mucosa
21	63	F	both sides	buccal mucosa		2	right	white	left	white	right	reticular	left	reticular	buccal mucosa**
22	73	F	right side	buccal mucosa		1	right	red			right	erosive			right buccal mucosa
23	75	F	both sides	buccal mucosa		2	right	red	left	red	right	erosive	left	erosive	left buccal mucosa
24	56	F	both sides	buccal mucosa		2	right	white	left	white	right	reticular	left	reticular	right buccal mucosa
25	70	F	both sides	buccal mucosa	lower both sides of gingiva	4	right	white	left	white	right	reticular	left	reticular	left buccal mucosa
26	67	F	right side	buccal mucosa		1	right	red			right	erosive and reticular			right buccal mucosa
27	71	F	both sides	buccal mucosa		2	right	red	left	red	right	reticular	left	atrophic	right buccal mucosa
28	54	F	left side	buccal mucosa		1			left	red			left	erosive and reticular	left buccal mucosa
29	60	F	both sides	buccal mucosa	left lateral border of tongue	3	right	red	left	white	right	reticular	left	reticular	right buccal mucosa
30	71	F	both sides	buccal mucosa		2	right	white	left	white	right	reticular	left	reticular	right buccal mucosa
31	71	F	both sides	buccal mucosa		2	right	white	left	white	right	reticular	left	reticular	buccal mucosa**
32	54	F	both sides	buccal mucosa		2	right	white	left	white	right	reticular	left	reticular	gingiva
33	56	F	left side	buccal mucosa		1			left	white			left	reticular	left buccal mucosa
34	69	F		lower lip	lower anterior of gingiva	2		red				erosive and reticular			lower lip
35	82	F	both side	buccal mucosa	upper both sides of gingiva, palate	5	right	red	left	red	right	reticular	left	reticular	right buccal mucosa
36	53	F	both side	buccal mucosa	upper both sides of gingiva	4	right	red	left	red	right	reticular	left	reticular	left buccal mucosa
37	49	F	both side	buccal mucosa	left lateral border of tongue	3	right	white	left	white	right	reticular	left	reticular	lateral border of tongue
38	75	F	both side	buccal mucosa		2	right	red	left	red	right	reticular	left	reticular	right buccal mucosa
39	78	F	both side	buccal mucosa		2	right	red	left	red	right	reticular	left	reticular	right buccal mucosa
40	58	F	both side	buccal mucosa		2	right	white	left	white	right	reticular	left	reticular	left buccal mucosa
41	59	F	both side	buccal mucosa		2	right	red	left	red	right	reticular	left	reticular	left buccal mucosa
42	72	F	both side	buccal mucosa	tip of tongue, lower lip,upper and lower both sides of gingiva	8	right	red	left	red	right	reticular	left	reticular	right buccal mucosa

* Number of affected sites

**Details of biopsy site is unknown

Table2 Clinico-pathological characteristics of all cases (Study 2: Hyper keratosis and fibro-epithelial polyp)

C.D.[a]	F-E polyp[c]		Hyperkeratosis							
P.D.[b]	Normal mucosa		Hyperplasia[d]		Low-grade dysplasia		High-grade dysplasia		OSCC[e]	
	Age	Sex	Age	Sex	Age	Sex	Age	Sex	Age	Sex
	47	M	42	M	61	M	65	M	72	M
	55	M	58	M	73	M	70	M	69	M
	63	M	65	M	68	M	60	M	66	M
	69	M	70	M	57	M	76	M	69	M
	64	M	73	M	69	M	67	F	64	M
	57	F	78	M	78	M	82	F	80	F
	61	F	56	F	70	F	64	F	73	F
	53	F	66	F	68	F	66	F	68	F
	63	F	73	F	61	F	78	F	78	F
	59	F	78	F	66	F	75	F	74	F
Average[f]	58.6		68.3		66.3		72.0		74.6	
S.D.[g]	3.8		9.5		3.9		7.3		4.7	

[a] Clinical diagnosis
[b] Pathological diagnosis
[c] Fibro-epithelial polyp
[d] Squamous cell hyperplasia
[e] Oral squamous cell carcinoma
[f] Average age
[g] Standard deviation

Table 3 Histopathogical and immunohistochemical (Study 1, 2)

	general staining	immunohistochemical staining primary antibody	
	hematoxylin and eosin (HE)	CD34 (QBEnd 10, 1:100; Dako)	SMA (1A4, 1:100; Dako)
Study 1: OLP	O		O
Study 2: OL and OSCC	O	O	

Table 4 Histopathological characteristics of all cases (Study 1: Oral lichen planus)

Case	Histopathological findings							
	Epithelium				Mesenchyme			
	Keratinization degree	Civatte body	Dyskeratosis	Rete pegs	Max Joseph spaces	Liquefaction degeneration	Melanin deposition	Micro hemorrhages
1	parakeratosis	○		serrated		○		○
2	parakeratosis			flat		○	○	
3	parakeratosis			serrated		○	○	
4	parakeratosis	○		flat		○		
5	parakeratosis	○	○	serrated		○		
6	parakeratosis		○	serrated		○	○	○
7	parakeratosis			serrated		○		○
8	parakeratosis			flat		○		
9	parakeratosis			serrated		○		○
10	parakeratosis			serrated		○	○	
11	parakeratosis			serrated		○		
12	parakeratosis			serrated		○	○	
13	parakeratosis			serrated		○		
14	parakeratosis	○		flat		○		
15	parakeratosis	○		serrated	○	○	○	
16	parakeratosis		○	serrated		○		○
17	parakeratosis	○		serrated		○	○	○
18	parakeratosis			flat		○	○	
19	parakeratosis			serrated	○	○		○
20	parakeratosis	○		serrated		○		
21	parakeratosis			serrated		○		
22	parakeratosis			flat		○		○
23	parakeratosis			serrated		○		
24	parakeratosis			serrated	○	○		○
25	parakeratosis	○		serrated		○	○	○
26	parakeratosis			serrated		○		
27	parakeratosis			serrated	○	○		○
28	parakeratosis			flat		○		
29	parakeratosis			flat		○		○
30	parakeratosis	○	○	serrated		○		
31	parakeratosis			serrated		○		
32	parakeratosis		○	flat	○	○	○	
33	parakeratosis			flat		○		
34	parakeratosis			flat		○		
35	parakeratosis	○		serrated		○		
36	parakeratosis			serrated		○	○	○
37	parakeratosis			serrated		○	○	
38	parakeratosis			serrated	○	○		
39	parakeratosis			serrated		○		
40	parakeratosis	○		serrated		○		
41	parakeratosis			flat	○	○	○	
42	parakeratosis			flat		○	○	